

Ca²⁺/Calmodulin Directly Interacts with the Pleckstrin Homology Domain of AKT1^{*[5]}

Received for publication, March 12, 2007, and in revised form, June 4, 2007. Published, JBC Papers in Press, June 19, 2007, DOI 10.1074/jbc.M702123200

Biao Dong¹, C. Alexander Valencia¹, and Rihe Liu²

From the School of Pharmacy and Carolina Center for Genome Sciences, University of North Carolina, Chapel Hill, North Carolina 27599

AKT kinase, also known as protein kinase B, is a key regulator of cell growth, proliferation, and metabolism. The activation of the AKT signaling pathway is one of the most frequent molecular alterations in a wide variety of human cancers. Dickson and coworkers recently observed that Ca²⁺-calmodulin (Ca²⁺-CaM) may be a common regulator of AKT1 activation (Deb, T. B., Coticchia, C. M., and Dickson, R. B. (2004) *J. Biol. Chem.* 279, 38903–38911). In our efforts to scan the mRNA-displayed proteome libraries for Ca²⁺-CaM-binding proteins, we found that both human and *Caenorhabditis elegans* AKT1 kinases bound to CaM in a Ca²⁺-dependent manner (Shen, X., Valencia, C. A., Szostak, J., Dong, B., and Liu, R. (2005) *Proc. Natl. Acad. Sci. U. S. A.* 102, 5969–5974 and Shen, X., Valencia, C. A., Gao, W., Cotten, S. W., Dong, B., Chen, M., and Liu, R. (2007) submitted for publication). Here we demonstrate that Ca²⁺-CaM and human AKT1 were efficiently co-immunoprecipitated, and their interaction was direct rather than mediated by other proteins. The binding is in part attributed to the first 42 residues of the pleckstrin homology (PH) domain, a region that is critical for the recognition of its lipid ligands. The PH domain of human AKT1 can disrupt the complex of the full-length AKT1 with Ca²⁺-CaM. In addition, Ca²⁺-CaM competes with phosphatidylinositol 3,4,5-trisphosphate for interaction with the PH domain of human AKT1. Our findings suggest that Ca²⁺-CaM is directly involved in regulating the functions of AKT1, presumably by releasing the activated AKT1 from the plasma membrane and/or prohibiting it from re-association with phosphoinositides on plasma membrane.

AKT³ was originally discovered as an oncogene transduced by the acute transforming retrovirus (4, 5). It is now known to

include a family of three closely related members, namely AKT1, AKT2, and AKT3, each encoding a highly conserved serine/threonine protein kinase homolog (6, 7). The three AKT isoforms differ slightly in the localization of their regulatory phosphorylation sites. AKT1 is predominant in most tissues; AKT2 is highly expressed in insulin-responsive tissues; whereas AKT3 is abundant in brain tissues. AKT kinases consist of three conserved domains, including a pleckstrin homology (PH) domain at the N terminus, a kinase catalytic domain at the center, and a regulatory hydrophobic motif containing domain at the C terminus (8). The N-terminal PH domain spans from 1 to 107 amino acids and is ~80% identical among the AKT isoforms. The central catalytic domain is ~90% identical among the AKT isoforms and is closely related to protein kinase A, protein kinase C, glycogen synthase kinase-3, and S6 subfamilies of the AGC kinase family. This central domain catalyzes the phosphorylation of numerous AKT downstream substrates, including p21, glycogen synthase kinase-3, Bad, Forkhead, caspase-9, IKK, and Mdm2 (9–22). The C-terminal extension is ~70% identical among the three AKT isoforms and is most closely related to the protein kinase C family. It appears that this extension domain wraps around the front of the ATP binding pocket and interacts through a regulatory hydrophobic motif with a pocket at the back of the kinase domain.

The signaling pathway of AKT starts from the activation of phosphatidylinositol 3-kinase through binding of a growth factor to a receptor tyrosine kinase (23–26). The activated phosphatidylinositol 3-kinase converts membrane-bound PtdIns(3,4)P₂ to PtdIns(3,4,5)P₃. The PH domain of AKT then interacts with PtdIns(3,4,5)P₃, which results in anchoring the AKT kinase to the plasma membrane, where it undergoes phosphorylation and activation by 3-phosphoinositide-dependent protein kinase-1, the rictor-mammalian target of rapamycin complex, and probably other kinases (27, 28). AKT is fully activated following its phosphorylation at two regulatory residues, which are structurally and functionally conserved within the AGC kinase family. These residues include a threonine residue on the kinase catalytic domain (Thr-308, Thr-309, and Thr-305 for AKT1, AKT2, and AKT3, respectively) and a serine residue

* This work was supported by start-up funds from the Carolina Center for Genome Sciences and School of Pharmacy at the University of North Carolina at Chapel Hill (to R.L.), National Institutes of Health Grant R21DK067480 (to R.L.), and American Cancer Society Research Scholar Grant RSG-06-073 (to R.L.). The costs of publication of this article were defrayed in part by the payment of page charges. This article must therefore be hereby marked "advertisement" in accordance with 18 U.S.C. Section 1734 solely to indicate this fact.

[5] The on-line version of this article (available at <http://www.jbc.org>) contains supplemental Figs. S1–S3.

¹ Both authors contributed equally to this work.

² To whom correspondence should be addressed: School of Pharmacy, CB# 7360, Beard Hall 209, University of North Carolina, Chapel Hill, NC 27599. Tel.: 919-843-3635; Fax: 919-968-0081; E-mail: rliu@email.unc.edu.

³ The abbreviations used are: AKT, protein kinase B; PH, pleckstrin homology; CaM, calmodulin; CALNA, Ca²⁺/calmodulin-dependent protein phosphatase or calcineurin A; CaMK, Ca²⁺/calmodulin-dependent protein kinase; CaMKK, Ca²⁺/calmodulin-dependent protein kinase kinase; GST, glutathi-

one S-transferase; IKK, IκB kinase; Mdm2, mouse double minute 2 protein; MLCK, myosin light chain kinase; PtdIns(3,4,5)P₃, phosphatidylinositol 3,4,5-trisphosphate; PtdIns(3,4)P₂, phosphatidylinositol 3,4-bisphosphate; PtdIns(3,5)P₂, phosphatidylinositol 3,5-bisphosphate; PtdIns(4,5)P₂, phosphatidylinositol 4,5-bisphosphate; SNAP25, synaptosomal-associated protein, 25 kDa; TNT, coupled *in vitro* transcription and translation; PIP, phosphatidylinositol phosphate; PIP₂, phosphatidylinositol bisphosphate; PIP₃, phosphatidylinositol 3,4,5-trisphosphate.



Interaction between Ca^{2+} /CaM and the PH Domain of AKT1

on the hydrophobic motif (Ser-473, Ser-474, and Ser-472 for AKT1, AKT2, and AKT3, respectively). Such activation permits a conformational change that results in substrate binding and a significant increase of the rate of catalysis.

AKT family members regulate a wide variety of cellular functions, including apoptosis, cellular proliferation, differentiation, intermediary metabolism, genome stability, and neo-vascularization (25, 27). The regulation mechanism of AKT is by deactivation or activation of its downstream substrates through phosphorylation. For instance, AKT kinase facilitates growth factor-mediated cell survival and blocks apoptotic cell death by phosphorylating and deactivating pro-apoptotic factors such as Bad, caspase-9, and Forkhead transcription factors (9, 14–19). AKT also phosphorylates and inactivates glycogen synthase kinase-3, which allows the activation of glycogen synthase (13). On the other hand, AKT phosphorylates and activates IKK α , which phosphorylates I κ B followed by its ubiquitination and proteasomal degradation (20–22, 29). AKT regulates many cellular processes that, upon deregulation, may contribute to the development or progression of cancer. It is now evident that the activation of the AKT signaling pathway is one of the most frequent molecular alterations in a wide variety of human cancers (30–34). Overexpression or inappropriate activation of AKT1 is noted in many types of cancer.

Despite its importance in numerous signaling pathways, our understanding of the activation and regulation of AKT kinases is still incomplete. The lipid-binding PH domain of AKT plays an important role in promoting the translocation of AKT to the plasma membrane for activation. Recent results suggest that the PH domain is also important for the interaction with a number of other proteins (35). In our recent effort to scan the mRNA-displayed proteome libraries for Ca^{2+} -CaM-binding proteins, we found that both human and *Caenorhabditis elegans* AKT1 bound to CaM in a Ca^{2+} -dependent manner (2).⁴ Here we extend Dickson's work and report that AKT1 interacts with Ca^{2+} -CaM through two binding motifs, one at the first half of the N-terminal PH domain and another at the N terminus of the kinase catalytic domain. Our results indicate that Ca^{2+} -CaM and AKT1 can be co-immunoprecipitated and the Ca^{2+} -CaM binding appears to be general in all three AKT isoforms. The Ca^{2+} -CaM binding to the N-terminal PH domain of AKT1 could regulate its interaction with PtdIns(3,4,5)P₃.

EXPERIMENTAL PROCEDURES

Construction of Recombinant Genes and Expression of AKT1 Fragments—The cDNA corresponding to the open reading frame of human AKT1 was reversibly transcribed from a human poly(A)⁺ mRNA library (Ambion, Austin, TX). The full-length AKT1 was amplified using a high fidelity Platinum Pfx DNA polymerase (Invitrogen) with the following primers: forward primer, 5'-CACCATGAGCGACGTGGCTATTGTGA-3'; reverse primer, 5'-GGCCGTGCCGCTGGC-3'. The PCR product of full-length AKT1 was gel-purified and cloned into a pcDNA3.1/V5-His TOPO vector (Invitrogen)

according to the manufacturer's instructions. The resulting AKT1-containing plasmid was confirmed by PCR and sequence analysis. This construct was used as the template to PCR-amplify various AKT1 fragments.

The synthesis of AKT1 fragments using coupled *in vitro* transcription and translation (TnT) was performed as previously described (2). The primers for the generation of the PCR products of these AKT1 fragments were as follows. For the fragment F_{43–115}, BD-HS43-5 (5'-CAATTACTATTACAATTACAATGGGACAGGATGTGGACCAAC-3') and BD-HS115-3 (5'-TTAATGGTGATGGTGATGATGCTCCCTCTGCTTCTTGAGGC-3'); for F_{116–149}, BD-HS116-5 (5'-CAATTACTATTACAATTACAATGGGAGAGGAGATGGACTTCC-3') and BD-HS149-3 (5'-TTAATGGTGATGGTGATGATGCTCGTTCATGGTCACGCGG-3'); for F_{150–197}, BD-HS150-5 (5'-CAATTACTATTACAATTACAATGGGATTTGAGTACCTGAAGCTG-3') and BD-HS197-3 (5'-TTAATGGTGATGGTGATGATGGGTGAGTGTGTGGGCCAC-3'); for F_{198–408}, BD-HS198-5 (5'-CAATTACTATTACAATTACAATGGGAGAGAACC GCGTCC-3') and BD-HS408-3 (5'-TTAATGGTGATGGTGATGATGAAA GAAGCGATGCTGCATGATCTC-3'); for F_{409–480}, BD-HS409-5 (5'-CAATTACTATTACAATTACAATGGGAGCCGGTATCGTGTG-3') and BD-HS480-3 (5'-TTAATGGTGATGGTGATGATGGGCCGCTGCCGCTGGC-3'); for F_{1–115}, BD-HS1-5 (5'-CAATTACTTTTACAATTACAATGGGAAGCACGTGGCTATTG-3') and BD-HS115-3; for F_{1–149}, BD-HS1-5 and BD-HS149-3; for F_{1–408}, BD-HS1-5 and BD-HS408-3; for F_{1–480}, BD-HS1-5 and BD-HS480-3; for F_{150–408}, BD-HS150-5 and BD-HS408-3; for F_{150–480}, BD-HS150-5 and BD-HS480-3; and for F_{116–480}, BD-HS116-5 and BD-HS480-3.

Some fragments were also overexpressed and purified as GST fusion proteins in *Escherichia coli*. The primers are: for F_{1–42}, HS-3-F (5'-GACGACGACAAGATGAGCGACGTGGCTATTGTGA-3') and HS-3-R (5'-GAGGAGAAGCCCGGT-TTACGGCCGCTCCTGTAGC-3'); for F_{1–115}, HS-3-F and HS-1-R (5'-AGGAGAAGCCCGGTTTACTCCTCCTGCTTCTTGAGG-3'); for F_{92–115}, HS-1-F (5'-GACGACGACAAGATGACTCCTGAGGAGCGGG-3') and HS-1-R; for F_{116–197}, HS-2-F (5'-GACGACGACAAGATGGAGGAGATGGACTTCCGG-3') and HS-2-R. The sequences corresponding to these fragments were cloned into an expression vector pET-41 EK/LIC containing an N-terminal GST tag (Novagen, Madison, WI). After confirmation of sequences, the insert-containing plasmids were transformed into BL21(DE3)-competent cells for expression of various AKT1 fragments. Soluble protein fragments were purified using glutathione-agarose beads (Santa Cruz Biotechnology, Santa Cruz, CA) according to the manufacturer's instructions.

Purified PH domain (residues 1–149), PH domain-deleted AKT1 (residues 118–480, active), full-length human AKT1 (residues 1–480, both active and inactive), full-length AKT2, and full-length AKT3 were purchased from Upstate (Charlottesville, VA). The PH domain-deleted AKT1 (residues 140–480) from New England Biolabs (Ipswich, MA) was also used.

Cell Culture and Lysate Preparation—HeLa S3 cells were grown to stationary phase in Ham's F-12 medium supple-

⁴X. Shen, C. A. Valencia, W. Gao, S. W. Cotten, B. Dong, M. Chen, and R. Liu, submitted for publication.

mented with 10% fetal bovine serum. Cells were harvested and lysed as reported (36). After centrifugation to remove intact cells, the supernatants were cleared at 14,000 rpm for 15 min at 4 °C. Lysates prepared were used for pulldown assays and co-immunoprecipitation experiments.

CaM Binding and Pulldown Assays—To investigate the interaction between Ca^{2+} -CaM and fragment/full length AKT, CaM binding assays were performed using both radiolabeled AKT protein fragments generated by TNT and GST-tagged fragments overexpressed in *E. coli*. For the TNT approach, radiolabeled AKT fragments were synthesized in the presence of 10 μCi of [^{35}S]methionine (PerkinElmer Life Sciences) in a total volume of 25 μl for 90 min at 30 °C as previously described (2). To perform the CaM binding assays, an aliquot of the TNT product was mixed with an appropriate amount of biotinylated CaM for 90 min at 4 °C in buffer A (25 mM Tris-HCl, pH 8.0, 150 mM NaCl, 1 mg/ml bovine serum albumin, 5 mM 2-mercaptoethanol, 1 mM CaCl_2) or buffer B (same as buffer A except 1 mM CaCl_2 was replaced with 2 mM EGTA). After binding, 30 μl of the 50% slurry of streptavidin beads (Pierce Biotech, Rockford, IL) was added, and the mixture was incubated for 45 min at room temperature with gentle mixing. The supernatant was removed by centrifugation in an Ultrafree-MC centrifugal filter tube (Millipore, Billerica, MA), and the beads were washed three times with 150 μl of buffer A. Proteins captured were then released from the column by chelating Ca^{2+} with 150 μl of buffer B. Each fraction was separated by SDS-PAGE and images were obtained through a Storm 860 PhosphorImager.

When GST-tagged, overexpressed AKT fragments or cell lysates were used for the binding reaction, CaM-Sepharose pulldown assays were performed. To do that, 100 μl of pre-equilibrated CaM-Sepharose 4B beads (Amersham Biosciences) was added to an appropriate amount of purified AKT protein (1–10 μg), or HeLa S3 cell lysates (~1 mg of total protein), followed by incubation at 4 °C for 2–3 h in a buffer containing 50 mM Tris-HCl, pH 7.4, 150 mM NaCl, 1 \times EDTA-free protease inhibitor mix, with 1 mM Ca^{2+} (buffer C) or 2 mM EGTA (buffer D). The beads were washed three times with buffer C or buffer D. Proteins bound to CaM were eluted from the beads with buffer D. Proteins from each fraction (L, purified AKT protein or lysate; FT, flow-through; W, last wash before elution; and E, elution) were resolved on SDS-PAGE gels, transferred to a nitrocellulose membrane (Amersham Biosciences), and probed with either anti-AKT1 (Santa Cruz Biotechnology, Santa Cruz, CA), anti-His tag (R&D Systems, Minneapolis, MN), anti-AKT (for all AKT isoforms, Cell Signaling Technology, Danvers, MA), or anti-Calcieneurin A2 (Santa Cruz Biotechnology).

Competitive Binding and Elution Assay—For competitive binding experiments, 2 μM GST-tagged PH domain of AKT1 (Upstate) was added to a binding mixture with the full-length AKT1 pre-complexed with Ca^{2+} -CaM immobilized on Sepharose beads. The elution was performed with buffer B. For competitive elution experiments, 2–50 μM PH domain of AKT1 or a CaM-binding peptide from MLCK (Ac-RRKWQKT-GHAVRAIGRL-NH₂) (Calbiochem) in buffer A was used to elute the full-length AKT1 pre-complexed with Ca^{2+} -CaM on agarose beads.

CaM Binding Affinity Measurement—To measure the binding affinity of AKT fragments with Ca^{2+} -CaM, the [^{35}S]methionine-labeled PH domain F_{1–149}, F_{150–408}, and full-length AKT1 were generated by TNT and mixed with biotinylated CaM, whose concentration was varied in the range of 10 nM and 2.5 μM . Biotin-CaM-protein complex was captured by streptavidin beads, and the extent of binding was determined by scintillation counting of each fraction, followed by fitting the data to a binding curve using SIGMAPLOT 8.0 software (Systat, Richmond, VA).

Immunoprecipitation and Co-immunoprecipitation—Immunoprecipitation was performed by incubating 1 mg of HeLa S3 lysate with anti-CaM, anti-AKT1, or an irrelevant IgG, respectively. Samples were separated by SDS-PAGE, transferred to a nitrocellulose membrane, and probed with different antibodies.

For co-immunoprecipitation experiments, equal amounts of pre-cleared HeLa S3 whole cell lysate (~1 mg of total protein) were incubated with 2–5 μg of primary antibody (anti-CaM) for 4 h at 4 °C, in the presence of either buffer C or buffer D. 20 μl of pre-equilibrated protein A/G-agarose conjugate was added, and the mixture was further incubated at 4 °C for 2 h with mixing. The pellets were collected and washed three times with buffer C or D. After the final wash, pellets were eluted with buffer D. Different fractions were loaded onto SDS-PAGE followed by Western blotting and probing using anti-AKT1. Conversely, anti-AKT1 was used for co-immunoprecipitation and blots were probed with anti-CaM. As a positive control, blots were probed with anti-Calcieneurin A2, for the detection of calcineurin, a well known CaM-binding protein. As a negative control, blots were also probed with an irrelevant anti-TFII antibody.

Protein Lipid Overlay Assay—PtdIns(3,4,5)P₃, PtdIns(3,4)P₂, PtdIns(3,5)P₂, PtdIns(4,5)P₂, and phosphatidylcholine were obtained from Echelon Biosciences (Salt Lake City, UT). 100 pmol of each PIP were dotted on a Hybond-C Extra membrane (Amersham Biosciences), and protein lipid overlay assay was performed according to the manufacturer's instructions. Different amounts of PtdIns(3,4,5)P₃ were also used to examine its concentration dependence. The membrane was first blocked for 1 h in a TBS buffer (25 mM Tris-HCl, pH 8.0, 150 mM NaCl) with 0.1% (v/v) Tween 20 and 3% (w/v) bovine serum albumin. It was then incubated at 4 °C overnight with 0.5 $\mu\text{g}/\text{ml}$ His-tagged full-length AKT1 (Upstate), GST-tagged PH domain of AKT1 (Upstate), or His-tagged AKT1 without PH domain (Upstate) in the blocking buffer containing 0.24 μM CaM and 100 μM Ca^{2+} or EGTA. After washing three times, the membrane was incubated with anti-His tag or anti-GST for 3 h at room temperature. The membrane was washed again and incubated with anti-mouse IgG horseradish peroxidase (Amersham Biosciences), followed by development using ECL plus Western blotting detection system (Amersham Biosciences).

RESULTS

To address the difficulty of identifying the numerous conditional interactions that are dependent on the intracellular Ca^{2+} concentrations, we developed an mRNA-display protein selection platform that allows us to scan a proteome of interest for

Interaction between Ca²⁺/CaM and the PH Domain of AKT1



FIGURE 1. Schematic presentation of the Ca²⁺-CaM-binding AKT1 fragments selected from an mRNA-displayed *C. elegans* proteome library. The region of the PH domain of *C. elegans* AKT1 is indicated with arrows.

Ca²⁺-dependent protein-protein interactions (2).⁴ By employing this novel approach, we have scanned both the human and the *C. elegans* proteomes for Ca²⁺-CaM-binding proteins (2).⁴ A large number of both known and previously uncharacterized Ca²⁺-CaM-binding proteins were identified, including many protein kinases. These CaM-binding kinases include CaM-dependent protein kinase, CaM-dependent protein kinase kinase, elongation factor kinase, and protein kinase C family member UNC-13 that have been previously characterized to interact with Ca²⁺-CaM (37). Several protein kinases that have not been previously reported to interact with Ca²⁺-CaM were also identified, and AKT1 is among them. The discovery that both human and *C. elegans* AKT1 kinases interact with CaM in a Ca²⁺-dependent manner strongly suggests that Ca²⁺-CaM play an important role in regulating the functions of AKT.

We first characterized the interaction of Ca²⁺-CaM with AKT1 by sequence analysis of the selected fragments. Only one fragment originating from human AKT1 was isolated in the Ca²⁺-CaM-binding selection using an mRNA-displayed human proteome library. Sequence analysis showed that this was a fragment that covered the entire PH domain of human AKT1. However, four fragments originating from *C. elegans* AKT1 were isolated, namely, F₁₋₁₄₄, F₅₄₋₁₃₈, F₁₀₅₋₁₃₈, and F₁₀₃₋₁₇₂ (Fig. 1). All these fragments are located within or close to the PH domain of *C. elegans* AKT1. F₁₋₁₄₄ contains the whole PH domain (the arrowed region), whereas F₅₄₋₁₃₈ contains its second half. The shortest overlapping region is between residues 105 and 138 (¹⁰⁵VRQRWIHAIESISKKYKGTNANPQEELMETNQQP¹³⁸). This region covers the C-terminal part of the PH domain and part of the LINK region. Using a web-based motif analysis program (37), it is found that this fragment contains a positively charged amphiphilic α -helix (underlined), which is a characteristic of many Ca²⁺-CaM binding motifs.

To investigate the interaction of these fragments with CaM, we generated radiolabeled AKT fragments by TNT and used them in the CaM binding assay in the presence or absence of Ca²⁺. We first validated the assay using both positive and negative controls. For positive controls, more than 20 well known human Ca²⁺-CaM-binding proteins or their fragments con-

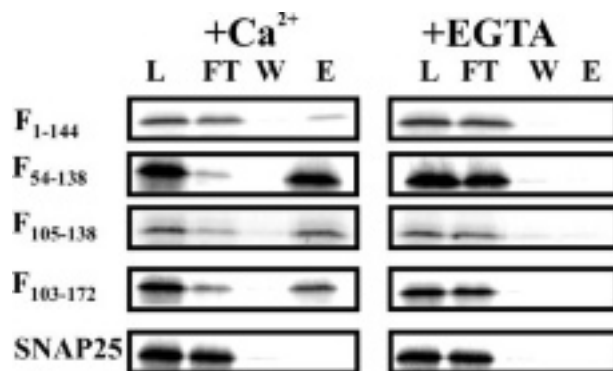


FIGURE 2. *In vitro* Ca²⁺-CaM binding of AKT1 fragments selected from an mRNA-displayed *C. elegans* proteome library. [³⁵S]Methionine-labeled protein fragments were generated by TNT. An aliquot of the TNT reaction mixture was incubated with an appropriate amount of biotinylated CaM in the presence or absence of Ca²⁺, followed by mixing with streptavidin-agarose beads. The beads were washed, and the bound proteins were eluted using a buffer containing EGTA. Each fraction was separated by SDS-PAGE, and images were obtained by autoradiography. Numerous positive and negative controls were performed but only SNAP25 was shown here as a negative control. L, TNT product; FT, flow through; W, last wash before elution; and E, elution.

taining the Ca²⁺-CaM binding motifs were synthesized by TNT and used to test their CaM binding with this assay. It was found that all these positive controls bound to CaM specifically in a Ca²⁺-dependent manner (data not shown). For negative controls, a number of proteins or their fragments that have never been reported to interact with CaM were used. In addition, several known Ca²⁺-CaM-binding proteins with the Ca²⁺-CaM binding motifs deleted were also used as negative controls. No binding was detected for these negative control proteins under the conditions used in such *in vitro* assay, as shown in Fig. 2 using SNAP25 as an example. The results of both positive and negative controls demonstrate this CaM binding assay is a very robust method to elucidate protein interactions with Ca²⁺-CaM. Using this CaM binding assay, it was found that all the four selected *C. elegans* AKT fragments bound to CaM in a Ca²⁺-dependent manner as shown in Fig. 2, and the binding was completely abolished when Ca²⁺ was chelated with EGTA. When irrelevant proteins such as SNAP25 were used as negative controls, no CaM binding was observed. Interestingly, F₅₄₋₁₃₈, a fragment that covers both the second half of the PH domain and the LINK region, bound to Ca²⁺-CaM very tightly, implying it contains at least one of the major binding motifs. It appears that the interaction of Ca²⁺-CaM with the longer fragment F₁₋₁₄₄ was not as strong as that with F₅₄₋₁₃₈ or F₁₀₅₋₁₃₈. This phenomenon was also observed in the interaction of CaM with a number of other proteins (2), presumably because the CaM binding motifs are more accessible when present as short fragments.

Because the antibodies for *C. elegans* AKTs are not readily available, we focused our investigation on human AKTs. We hypothesized that human AKTs should use different region(s) at or close to the PH domain to interact with Ca²⁺-CaM, presumably because the LINK region of *C. elegans* AKT1 has very low sequence homology with human AKT1 (supplemental Fig. S1). To map the location of the CaM binding motif(s) on human AKT1, we generated by TNT [³⁵S]methionine-labeled protein fragments that cover all the possible regions of AKT1 (Fig. 3).

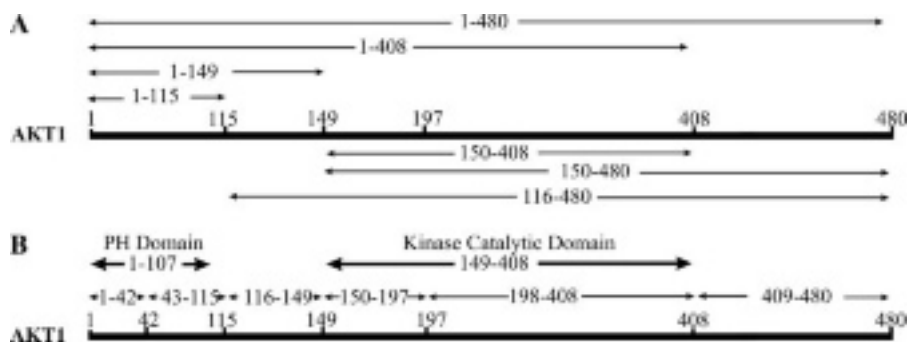


FIGURE 3. Schematic diagram of the overexpressed human AKT1 fragments used in mapping the Ca^{2+} -CaM binding motifs. Different regions on full-length human AKT1 are indicated with arrows. *A*, list of fragments that are relatively longer; *B*, list of fragments that are shorter.

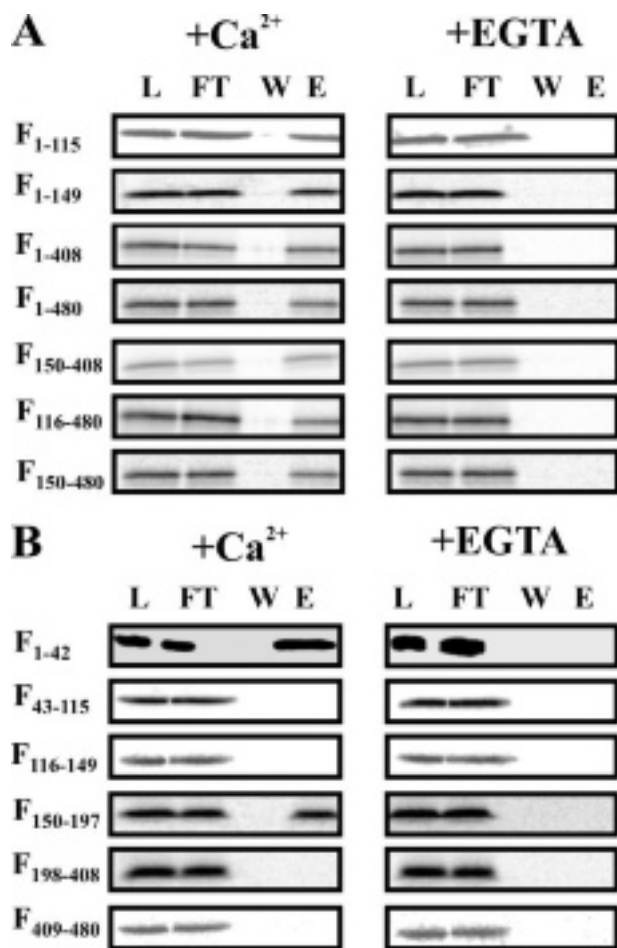


FIGURE 4. *In vitro* CaM binding assays using different human AKT1 fragments. All the fragments were generated by TNT, except F_{1-42} , which could not be TNT-synthesized and was obtained by overexpression in *E. coli*. For TNT-generated fragments, an appropriate amount of [^{35}S]methionine-labeled AKT1 fragment was incubated with biotinylated CaM in a buffer containing either Ca^{2+} or EGTA. The beads were washed, and the bound molecules were eluted using a buffer containing EGTA. The fragments were separated by SDS-PAGE and detected by autoradiography. For F_{1-42} , the pull-down assay was performed with CaM-Sepharose in the presence of either Ca^{2+} or EGTA as detailed under "Experimental Procedures." F_{1-42} was detected by Western blot analysis using anti-GST. *L*, AKT protein fragment; *FT*, flow-through; *W*, last wash before elution; and *E*, elution. *A*, list of fragments that are relatively longer; *B*, list of fragments that are shorter.

Specifically, F_{1-115} covers the PH domain, $F_{116-149}$ the LINK region, $F_{150-408}$ the kinase catalytic domain, and $F_{409-480}$ the C-terminal extension domain, respectively. Consistent with the

result from the selection using an mRNA-displayed human proteome library, the PH domain of AKT1 (residues 1–115) bound to CaM well (Fig. 4A). This interaction is highly dependent on the presence of Ca^{2+} . When EGTA was included, the binding was completely abolished. All the fragments that contain the PH domain, including F_{1-149} , F_{1-408} , and F_{1-480} , also bound to CaM in a Ca^{2+} -dependent manner (Fig. 4A). We further mapped the binding motif within the PH

domain using F_{1-42} and F_{43-115} that cover two different parts of the PH domain. It appeared that the Ca^{2+} -CaM binding of the PH domain of AKT1 could be attributed to the first 42 residues, because F_{1-42} strongly bound to Ca^{2+} -CaM, whereas F_{43-115} showed no binding at all (Fig. 4B).

We then examined whether the PH domain-deleted AKT1 also interacted with Ca^{2+} -CaM. Surprisingly, $F_{116-480}$ also bound to Ca^{2+} -CaM (Fig. 4A), suggesting the presence of another CaM binding motif. To map this second binding motif, three protein fragments that cover the LINK region ($F_{116-149}$), the kinase catalytic domain ($F_{150-408}$), and the C-terminal extension domain ($F_{409-480}$), respectively, were generated and used to interact with CaM. Interestingly, it was found that this second CaM-binding site was not in the LINK or the C-terminal extension regions, but within the kinase catalytic domain. We further mapped this CaM binding motif to $F_{150-197}$ (Fig. 4B), a region at the N terminus of the kinase catalytic domain. Indeed, all the fragments that contain $F_{150-197}$ also bound to Ca^{2+} -CaM, including $F_{150-408}$, $F_{150-480}$, and $F_{116-480}$ (Fig. 4A). As already shown in Fig. 2, negative control proteins did not bind to CaM in these assays.

The results using TNT-generated protein fragments were consistent with the CaM-Sepharose pulldown assay using GST-tagged proteins overexpressed in *E. coli* (supplemental Fig. S2). To rule out the possibility of nonspecific interaction due to the presence of GST tag in such a pulldown assay, overexpressed GST alone was used in the binding. No binding was detected between GST tag and CaM, both in the presence and absence of Ca^{2+} . Taken together, our results suggest that there exist two Ca^{2+} -CaM binding motifs on human AKT1, one at the first half of the PH domain (F_{1-42}) and the other at the N terminus of the kinase catalytic domain ($F_{150-197}$).

To analyze the interaction quantitatively, we determined the binding affinity of these two fragments of AKT1 with Ca^{2+} -CaM by varying the concentration of biotinylated CaM used in the CaM binding assay. The binding affinity for F_{1-149} and $F_{150-408}$ was $\sim 750 \pm 100$ nM and 500 ± 80 nM, respectively. The full-length AKT1 has an affinity similar to that of these fragments. This relatively weak interaction suggests that each binding motif might require the elevation of local Ca^{2+} concentration to effectively compete with many other CaM-binding proteins *in vivo*.

To investigate the interaction between AKT1 and Ca^{2+} -CaM under physiological conditions, we first tested whether the

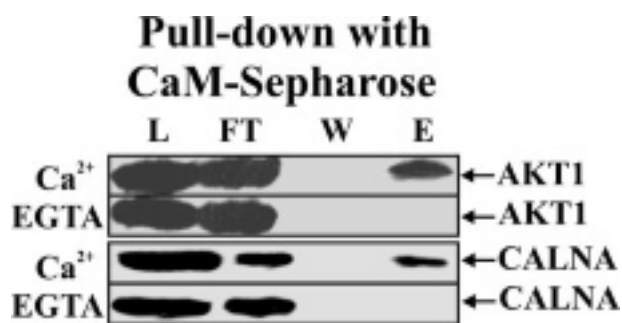


FIGURE 5. Pull-down assay of endogenous AKT1 from HeLa S3 cell lysate using CaM-Sepharose. The lysate was incubated with CaM-Sepharose 4B beads in the presence of either 1 mM CaCl_2 or 2 mM EGTA. The beads were washed, and the bound proteins were eluted with a buffer containing EGTA. Western blots were probed with anti-AKT1 for the presence of AKT1 or with anti-Calceinurin A2 for the presence of calcineurin as a positive control. L, lysate; FT, flow-through; W, last wash before elution; E, elution.

endogenous AKT1 could be pulled down by CaM-Sepharose. Fig. 5 shows that the AKT1 from human HeLa cells complexed with CaM in a Ca^{2+} -dependent fashion. When EGTA was present in the pull-down buffer, the binding of AKT1 to CaM-Sepharose was totally disrupted. As a positive control, a well known CaM-binding protein, calcineurin, was shown to bind to CaM through the pull-down assay. We further investigated whether the interaction exists *in vivo* by co-immunoprecipitation when both CaM and AKT1 are present at their physiological concentrations. Fig. 6A illustrates that AKT1 was co-immunoprecipitated with CaM when anti-CaM antibody was used for the immunoprecipitation. As a positive control, calcineurin was found to be co-immunoprecipitated with CaM as previously reported. As a negative control, we checked an irrelevant TFII protein and found it was not co-immunoprecipitated with CaM. Conversely, CaM was co-immunoprecipitated with AKT1 when anti-AKT1 was used in the immunoprecipitation (Fig. 6B). We also performed immunoprecipitation using an IgG and could not detect the presence of CaM or AKT1 by probing the Western blots using corresponding antibodies (data not shown). These results indicate that the AKT1- Ca^{2+} -CaM complex is present *in vivo*. Since direct binding of AKT1 with CaM has been detailed *in vitro*, the observed interaction with CaM is most likely to be direct rather than mediated by other proteins.

To investigate the possible role of CaM-binding on AKT1, we first examined whether the CaM binding motif near the N terminus of the kinase catalytic domain affects its kinase activity. To address this question, the phosphorylation of biotinylated cross-tide catalyzed by either active or inactive recombinant human AKT1 was performed in the presence of $[\gamma\text{-}^{32}\text{P}]\text{ATP}$. The kinase was preincubated with Ca^{2+} , Ca^{2+} -CaM, or EGTA/CaM, respectively, before being used in the phosphorylation reaction. Recombinant AKT1 proteins with PH domain deleted were also used in the assay. No change of phosphorylation was detected when Ca^{2+} -CaM was present (data not shown), indicating the catalytic activity of AKT1 is not regulated by CaM.

We then focused on examining the CaM binding motif at the PH domain of AKT1. To address this question, we investigated whether the interaction between Ca^{2+} -CaM and the full-length AKT1 could be disrupted by the free PH domain of AKT1.

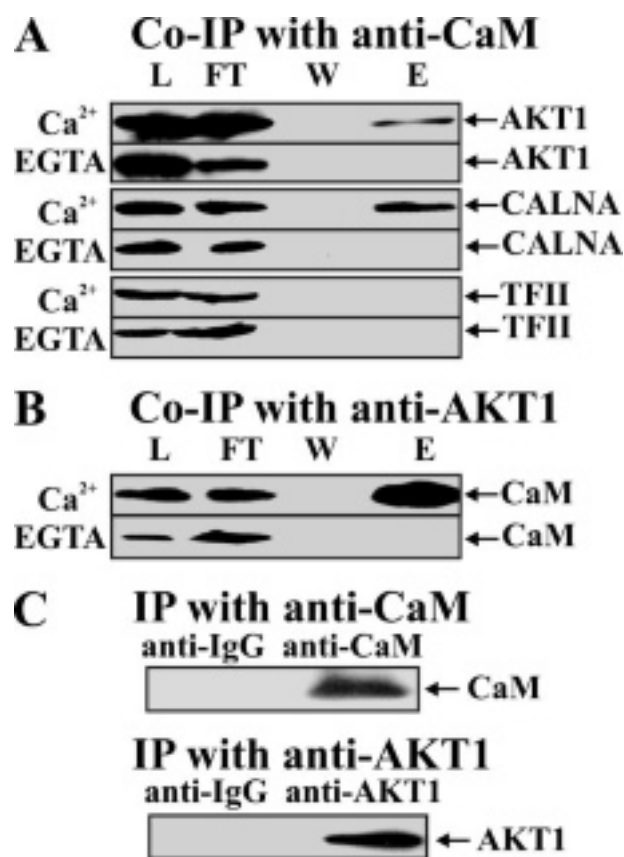


FIGURE 6. Co-immunoprecipitation of endogenous AKT1 from HeLa S3 cell lysate with CaM. Equal amounts of pre-cleared HeLa cell lysate were incubated with anti-CaM or anti-AKT1 antibody in the presence of either 1 mM CaCl_2 or 2 mM EGTA. The protein complex was captured by protein A/G-agarose conjugate and eluted with a buffer containing EGTA. A, co-immunoprecipitation with anti-CaM. Proteins associated with CaM were detected by Western blot analysis using anti-AKT1, anti-Calceinurin, and anti-TFII for AKT1, positive control protein (CALNA), and negative control protein (TFII), respectively. B, co-immunoprecipitation with anti-AKT1. CaM associated with AKT1 was detected by probing the Western blot with anti-CaM. C, immunoprecipitation controls showing that anti-CaM can capture CaM and anti-AKT1 can capture AKT1. L, lysate (not loaded proportionally); FT, flow-through; W, last wash before elution; E, elution.

Although the three-dimensional structure of the full-length AKT has not yet been reported, there exist several structures for the separate AKT and the PH domain (8, 38–41). It was modeled that the C-terminal helix of the PH domain extends about three turns beyond the consensus core, implying a well separated PH domain from the AKT catalytic region (8). We hypothesized that if the PH domain of AKT directly interacts with Ca^{2+} -CaM, the formation of the AKT- Ca^{2+} -CaM complex should be disrupted when a free PH domain of AKT is included in the binding mixture. Indeed, compared with that when no PH domain was added (Fig. 7A, panel 1), the amount of full-length AKT1 that could be pulled-down by CaM-Sepharose was significantly decreased when free PH domain was included in the binding buffer (Fig. 7A, panel 3), similar to that when the interaction was completely disrupted by chelating Ca^{2+} with EGTA (Fig. 7A, panel 2). This was presumably due to competitive binding from the externally added PH domain with CaM. Furthermore, it was found that the full-length AKT1 pre-complexed with Ca^{2+} -CaM could be eluted when an excess amount of free PH domain was used to replace EGTA in the elution

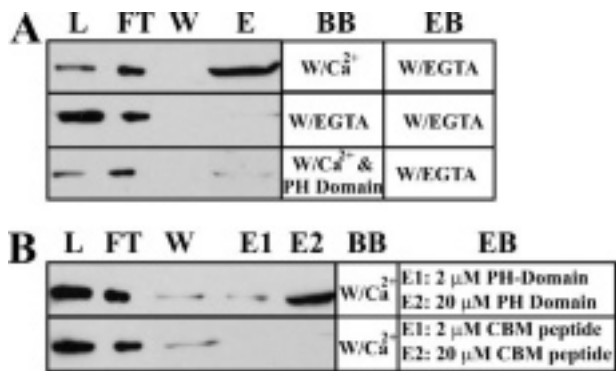


FIGURE 7. Competitive binding and competitive elution assays. *A*, competitive binding between CaM, full-length human AKT1 and PH domain of AKT1. 1 mM Ca^{2+} was included in the binding buffer (BB) to facilitate CaM binding (panels 1 and 3). 2 μM of the PH domain of AKT1 was added to the binding reaction mixture to compete with the full-length AKT1 for Ca^{2+} -CaM binding (panel 3). Panel 2 is a negative control in which the CaM binding was abolished by including EGTA in the binding buffer. Full-length AKT1 was eluted from CaM-Sepharose 4B beads with an elution buffer (EB) containing 0.5 mM EGTA. L, full-length AKT1 protein (not loaded proportionally); FT, flow-through; W, last wash before elution; E, elution with EGTA. *B*, competitive elution of full-length AKT1 pre-complexed with Ca^{2+} -CaM using the PH domain of AKT1 or MLCK peptide. Full-length AKT1 was first complexed with CaM on Sepharose 4B beads in the presence of Ca^{2+} . The bound AKT1 was then eluted by the PH domain of AKT1 (first panel) or MLCK peptide (second panel) twice with increased concentrations. L, full-length AKT1 protein (not loaded proportionally); FT, flow-through; W, last wash before elution; E1, first elution with 2 μM of PH domain of AKT1 or MLCK peptide; E2, second sequential elution with 20 μM of PH domain or MLCK peptide. Full-length AKT1 was detected by Western blot analysis using anti-AKT1.

buffer (Fig. 7B, panel 1). Significantly, a high concentration of free PH domain ($\sim 20 \mu\text{M}$) was required to elute the full-length AKT1, implying that the AKT1- Ca^{2+} -CaM complex is very stable once formed or that the second CaM binding site is contributing to the stabilization of the complex.

Although the amino acid sequences of the Ca^{2+} -CaM binding motifs in numerous CaM-binding target proteins are extremely diverse, many Ca^{2+} -CaM-binding proteins have one or more CaM-binding regions that are characterized by a basic amphipathic helix with ~ 20 amino acids in length, as that structurally detailed in myosin light chain kinase (MLCK) (37, 42). To determine if the PH domain of AKT1 competes with other CaM-binding proteins for the same binding region(s) on CaM, a short peptide from the CaM binding motif of MLCK was used to compete with full-length AKT1 in Ca^{2+} -CaM binding assay. This peptide was known to bind to Ca^{2+} -CaM with very high affinity ($K_d \sim 6 \text{ pM}$) (43). Surprisingly, unlike the PH domain, this Ca^{2+} -CaM-binding peptide could not competitively elute AKT1 from its complex pre-formed with Ca^{2+} -CaM (Fig. 7B, panel 2), indicating that the PH domain of AKT1 bind to Ca^{2+} -CaM at regions that are different from the conventional sites.

The PH domain of AKT is highly conserved among the three AKT isoforms (supplemental Fig. S3). Therefore, we examined whether other human AKT isoforms also interact with CaM in a similar fashion. Fig. 8 illustrates that CaM generally binds to AKT family members, including AKT2 and AKT3 in a Ca^{2+} -dependent manner. Significantly, all the binding with CaM was completely abolished when EGTA was used to chelate Ca^{2+} , indicating that Ca^{2+} -CaM complex is necessary for the observed interactions. Because the first 42 residues of the PH

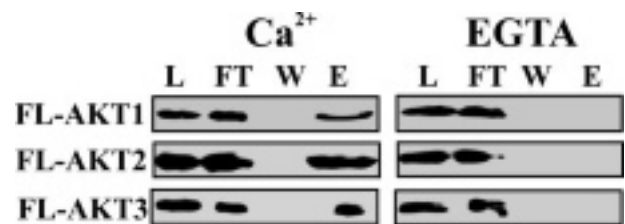


FIGURE 8. *In vitro* CaM-Sepharose pulldown assay using His-tagged full-length AKT1, AKT2, and AKT3. The pulldown assays were performed in the presence of either Ca^{2+} or EGTA. The AKT kinases were detected by Western blot analysis using anti-His tag. L, full-length AKT protein (not loaded proportionally); FT, flow-through; W, last wash before elution; E, elution with EGTA.

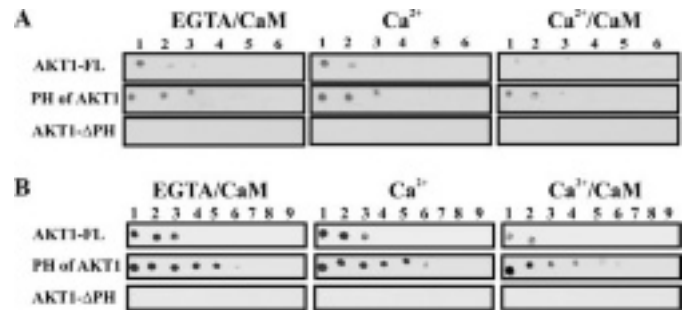


FIGURE 9. Protein lipid overlay assay. *A*, inhibition of the interaction of the PH domain of AKT1 with various phosphoinositides by Ca^{2+} -CaM. 100 pmol of each PIP was dotted on Hybond-C Extra membranes and pre-blocked with bovine serum albumin in TBS buffer. PIP strips were incubated with His-tagged full-length AKT1, GST-tagged PH domain of AKT1, or His-tagged AKT1 without PH domain in the presence of Ca^{2+} , EGTA/CaM, or Ca^{2+} -CaM, respectively. The proteins bound to the immobilized phosphoinositides on the membrane were detected using anti-His tag or anti-GST as the primary antibody and anti-mouse IgG-horseradish peroxidase as the secondary antibody. 1, PtdIns(3,4,5) P_3 ; 2, PtdIns(3,4) P_2 ; 3, PtdIns(4,5) P_2 ; 4, PtdIns(3,5) P_2 ; 5, phosphatidylcholine; 6, blank. *B*, inhibition of the interaction of the PH domain of AKT1 with various concentrations of PtdIns(3,4,5) P_3 by Ca^{2+} -CaM. The concentrations of PtdIns(3,4,5) P_3 dotted on the membrane were 200 pmol (lane 1), 100 pmol (lane 2), 50 pmol (lane 3), 25 pmol (lane 4), 13 pmol (lane 5), 6.3 pmol (lane 6), 3.2 pmol (lane 7), 1.6 pmol (lane 8), and 0 pmol (lane 9), respectively.

domain of AKT isoforms are $\sim 74\%$ identical (supplemental Fig. S3), it is likely that all three AKT isoforms interact with Ca^{2+} -CaM at the same regions through similar mechanism.

The major role of the PH domain of AKT is to recruit AKT from cytosol to plasma membrane through its interaction with PtdIns(3,4,5) P_3 . To address whether the interaction with Ca^{2+} -CaM affects the phosphoinositide-binding property of the PH domain of AKT, we first examined the complex formation between the PH domain of AKT1 and Ca^{2+} -CaM in the presence or absence of a phosphoinositide. It was found that the amount of the PH domain that could be pulled down by CaM-Sepharose was decreased $>60\%$ when PtdIns(3,4,5) P_3 was present (data not shown), implying that Ca^{2+} -CaM and PtdIns(3,4,5) P_3 directly compete for the PH domain of AKT. We further investigated whether the presence of Ca^{2+} -CaM disrupted the interaction between the PH domain of AKT and various phosphoinositides, using a protein lipid overlay assay. To this end, a strip membrane spotted with ~ 100 pmol of each PIP was used for the protein lipid overlay experiment with various amounts of full-length AKT1, the PH domain of AKT1, and AKT1 with PH domain deleted. Fig. 9A illustrates that the interactions between the PH domain of AKT1 and various phosphoinositides, including PtdIns(3,4,5) P_3 , PtdIns(3,4) P_2 ,

Interaction between Ca^{2+} /CaM and the PH Domain of AKT1

PtdIns(4,5) P_2 , and PtdIns(3,5) P_2 , were significantly reduced when Ca^{2+} ·CaM was included in the binding buffer. Such interruption of interaction between AKT1 and PIP was dependent on the concentrations of CaM used in the overlay assay (data not shown). The overlay assay was performed several times, and results were reproducible. The inhibition by Ca^{2+} ·CaM to each PIP was quantitatively analyzed by averaging the results from different overlay assays. For PtdIns(3,4,5) P_3 , Ca^{2+} ·CaM treatment lowered the full-length AKT1 binding from 100 to 20% when compared with EGTA/CaM treatment blot. Such interaction was not due to calcium, because there is no significant difference between Ca^{2+} and EGTA/CaM treatments in terms of the amount of full-length AKT1 binding to PtdIns(3,4,5) P_3 . For PtdIns(3,4) P_2 , the addition of Ca^{2+} ·CaM decreased the full-length AKT1 binding to 20% of EGTA/CaM and Ca^{2+} treatments. When the PH domain of AKT1 was used in the lipid overlay assay, its binding to PtdIns(3,4,5) P_3 decreased from 100% to 30% with the addition of Ca^{2+} ·CaM. Only ~20% of the PH domain of AKT1 bound to PtdIns(3,4) P_2 in the presence of Ca^{2+} ·CaM, compared with that with EGTA/CaM. Interestingly, PH domain of AKT1 bound to PtdIns(4,5) P_2 , but the binding was reduced to only 10% after the addition of Ca^{2+} ·CaM. No significant difference in terms of the amount of PH domain of AKT1 bound to each of the lipids was observed between EGTA/CaM- and Ca^{2+} -treated samples. Consistent with the findings reported in the literature, the interaction of AKT1 with phosphoinositides is PH domain-dependent, and was completely abolished when the PH domain was deleted from AKT1 protein (Fig. 9, panel 3). These results demonstrated that the interaction between the PH domain of AKT1 and phosphoinositides could be conditionally disrupted by CaM when the concentration of Ca^{2+} is elevated. We further examined the inhibition of the binding of the PH domain of AKT1 to a dilution series of PtdIns(3,4,5) P_3 by Ca^{2+} ·CaM. As shown in Fig. 9B, the inhibition is highly dependent on the PtdIns(3,4,5) P_3 concentrations. Although the interaction of the PH domain of AKT1 with PtdIns(3,4,5) P_3 was still clearly detected when PtdIns(3,4,5) P_3 was used at 13 pmol, the interaction was significantly inhibited by Ca^{2+} ·CaM in the whole concentration range.

DISCUSSION

Among a number of Ca^{2+} sensors in the eukaryotic cell, CaM is the most widespread and the best studied. CaM interacts with many different protein targets and mediates a wide variety of cellular functions. Most CaM-mediated signaling pathways are through the Ca^{2+} ·CaM complex, which is highly modulated by intracellular Ca^{2+} concentration (44–49). Two distinct CaM binding motifs on AKT1 were thoroughly mapped using protein fragments that cover all the possible regions of AKT1. In addition, those regions that contain a CaM binding motif were carefully examined using multiple smaller fragments, to further determine the location of the CaM binding motifs. Taken together, the observed CaM binding can be attributed to two well defined CaM-binding regions, one at the first half of the PH domain (F_{1-42}) and the other near the N terminus of the kinase catalytic domain ($F_{150-197}$). We found that all the fragments that contain one of the mapped CaM binding motifs bound to

CaM in a Ca^{2+} -dependent manner, whereas all the fragments that contain none of the mapped CaM binding motifs could not interact with CaM. Therefore, such CaM binding is less likely due to nonspecific interaction. Indeed, it is not unusual that CaM-binding proteins contain more than one CaM-binding domain, and the interactions of these proteins to CaM are well known to be specific (37). The presence of a second CaM binding motif near the N terminus of the catalytic domain of human AKT1 is intriguing. It appears that *C. elegans* AKT1 also contains a Ca^{2+} ·CaM binding motif close to this region. However, the exact location is different from that on human AKT1. Therefore, it is likely that AKT proteins from different species are regulated by Ca^{2+} ·CaM at close but not identical regions. It is also possible that this is not a function that has been conserved in *C. elegans*. The significance of the Ca^{2+} ·CaM binding motif near the N terminus of AKT1 catalytic domain remains to be determined. We found that the catalytic activity of human AKT1 was not affected by Ca^{2+} ·CaM. We postulate that the Ca^{2+} ·CaM regulation affects the activation or subcellular location of AKT1, rather than the kinase activity of the enzyme directly.

The PH domain of AKT has a β -barrel shape that is closed at one end by the C-terminal α -helix, whereas at the other end lie three loops that are variable, both in sequence and length, in all known PH domains (39). These loops form a highly basic pocket into which the 3- and 4-phosphates of PtdIns(3,4) P_2 and PtdIns(3,4,5) P_3 can bind. Specifically, before the binding of the lipid, the ligand-binding pocket in the PH domain is occupied by a complex hydrogen bonding network. Upon binding of a lipid such as Ins(1,3,4,5) P_4 , this network of hydrogen bonding is disrupted. In the 1–42 region, Tyr-18 moves away from the ligand-binding pocket to create space for the 5-phosphate, Glu-17 moves outwards to enable the contact of Arg-86 with the 4-phosphate, and Arg-23 moves inwards to make contact with the 1- and 3-phosphates. As for the residues close to the 1–42 region, a short acidic patch is formed through the clustering of three negatively charged residues (Asp-44, Asp-46, and Glu-49) upon ligand binding. We found that the binding of the PH domain of AKT1 could be in part attributed to residues 1–42 (Fig. 4). Because this region and its adjacent residues are critical in lipid ligand recognition, it is not surprising that the relatively weak interaction between the PH domain of AKT and the lipid ligands could be disrupted by Ca^{2+} ·CaM.

The PH domain is ~80% identical among the AKT isoforms, implying that other AKT isoforms also bind to Ca^{2+} ·CaM similar to AKT1. Indeed, AKT2 and AKT3 appear to interact with CaM in a manner that is highly dependent on Ca^{2+} . These results indicate that the interaction between Ca^{2+} ·CaM and the PH domain of AKT is not just limited to AKT1, but could be generally applied to all the three isoforms of AKT kinase. PH domains are found in many proteins involved in cellular signaling (50). However, AKT was the only PH domain-containing protein isolated from our Ca^{2+} ·CaM-binding selections using mRNA-displayed proteome libraries.

Our finding that AKT1 is a Ca^{2+} ·CaM-binding protein implies that the activity and functions of AKT1 are directly regulated by the calcium signal. It is well known that the activated AKT1 is released from the plasma membrane to switch

on or off a large number of signaling pathways. The mechanism of translocation of AKT1 to the plasma membrane for activation is well understood. Recently, the mechanism of deactivation of already activated AKT in cytosol was also revealed. It was found that PH domain leucine-rich repeat protein phosphatase could terminate already activated AKT by the dephosphorylation of its hydrophobic motif (51).

One question that has not yet been addressed is how the activated AKT is released or detached from the plasma membrane after activation by phosphorylation (55–57), and once detached, how to prohibit the activated AKT from re-association with $\text{PtdIns}(3,4,5)\text{P}_3$ on the plasma membrane. It is known that the level of $\text{PtdIns}(3,4,5)\text{P}_3$ on the plasma membrane is under control of lipid phosphatases, including SH2 domain-containing inositol 5'-phosphatase 2 and phosphatase and tensin homolog deleted on chromosome 10, that convert PIP_3 back to PIP_2 (52–54). Presumably, SH2 domain-containing inositol 5'-phosphatase 2 and phosphatase and tensin homolog deleted on chromosome 10 can only regulate the level of $\text{PtdIns}(3,4,5)\text{P}_3$ that are unbound to the PH domain, because it is difficult to understand how the already bound $\text{PtdIns}(3,4,5)\text{P}_3$ that forms extensive interactions with the PH domain of AKT could be accessed and further dephosphorylated by these lipid phosphatases. It is also known that the PH domain of AKT1 is not required for its activation or phosphorylation on Thr³⁰⁸ and Ser⁴⁷³. Conversely, based on the structural models of the full-length AKT, it is unlikely that the phosphorylation of two conserved residues at the well separated catalytic and extension domains of AKT significantly alters its interaction with $\text{PtdIns}(3,4,5)\text{P}_3$. The interactions between inositol phosphates and phosphoinositides to the PH domain of AKT have been investigated extensively (58–60). To understand the detachment of activated AKT from the plasma membrane, Hemmings and coworkers (57) proposed that the activated AKT might be detached from the membrane by competitive binding of inositol triphosphates such as $\text{Ins}(1,4,5)\text{P}_3$. However, it is known that $\text{Ins}(1,4,5)\text{P}_3$ binds to the PH domain of AKT with 3- to 5-fold lower affinity than $\text{PtdIns}(3,4)\text{P}_2$ or $\text{PtdIns}(3,4,5)\text{P}_3$, and other inositol phosphates bind to the PH domain at even lower affinities (58). Therefore, it is difficult to understand how the inositol triphosphate alone could efficiently detach the activated AKT from the plasma membrane.

Our finding that Ca^{2+} -CaM competes with $\text{PtdIns}(3,4,5)\text{P}_3$ and $\text{PtdIns}(3,4)\text{P}_2$ for interaction with the PH domain of AKT suggests a general mechanism of the regulation of AKT activation by CaM-mediated calcium signals. We propose that the membrane-bound AKT1 could be released from the plasma membrane and/or the released AKT could be further prohibited from re-association with $\text{PtdIns}(3,4)\text{P}_2$ on plasma membrane by CaM when local Ca^{2+} -CaM concentration is elevated. Because the intracellular concentration of Ca^{2+} -free CaM is high (47), this detachment process is likely coupled with the release of Ca^{2+} from intracellular storage by $\text{Ins}(1,4,5)\text{P}_3$, which results in a significant increase of local Ca^{2+} -CaM concentration. Unlike inositol phosphates and phosphoinositides that bind to their targets weakly, Ca^{2+} -CaM strongly interacts with

its targets, typically at a nanomolar scale. Although the affinity of the PH domain with Ca^{2+} -CaM reported here is ~ 750 nM, the interaction is still stronger than that with $\text{Ins}(1,4,5)\text{P}_3$. Indeed, it appears that the AKT-Ca^{2+} -CaM complex is very stable once formed (Fig. 7B, panel 1). Therefore, Ca^{2+} -CaM could efficiently detach the activated AKT from the plasma membrane or/and lock the PH domain of AKT to prohibit it from re-association with less abundant $\text{PtdIns}(3,4,5)\text{P}_3$ or abundant $\text{PtdIns}(3,4)\text{P}_2$ on the plasma membrane.

In this report, we demonstrate that Ca^{2+} -CaM directly and specifically interacts with the PH domain of AKT1 under *in vitro* conditions. The fact that AKT1 could be co-immunoprecipitated with CaM in a Ca^{2+} -dependent manner indicates that the AKT1/Ca^{2+} -CaM complex is present *in vivo* under physiological conditions. This work is an extension of that reported by Dickson and coworkers. Although we did not show that modulation of intracellular calcium affects AKT activity under physiological conditions, the original report demonstrated that EGF-induced AKT1 activation and survival in transgenic mouse mammary tumor virus-c-Myc mouse mammary carcinoma cells were both Ca^{2+} -CaM-dependent (1). Interestingly, such activation was mediated neither by CaM kinases nor by phosphatidylinositol 3-kinase, but was rather abolished by the intracellular Ca^{2+} chelator BAPTA-AM and by the specific CaM antagonist W-7. Furthermore, the AKT1 activation by serum and insulin was also inhibited by W-7, suggesting that the role of Ca^{2+} -CaM in the activation of AKT1 could be general and irrespective of upstream receptor activator, mammalian species, and transformation status. Such inhibition of AKT1 activation by intracellular Ca^{2+} chelator and specific CaM antagonist provided direct and strong evidence that the modulation of intracellular Ca^{2+} affects AKT1 activity under physiological conditions. These *in vivo* observations are consistent with our findings and support the hypothesis that Ca^{2+} -CaM regulates the function of AKT through interacting with its N-terminal PH domain. However, more *in vivo* work is crucial to further confirm this hypothesis in the cellular context.

AKT kinases are involved in numerous signaling pathways and regulated by different mechanisms. In addition to its interaction with $\text{PtdIns}(3,4,5)\text{P}_3$ to promote the translocation of the kinase to the plasma membrane, the PH domain of AKT also functions as a protein-protein interaction motif. It has been reported that the PH domain of AKT is involved in the oligomerization of AKT and is also important for interaction with a number of other proteins that are involved in the regulation of AKT, including TCL1, JIP1, Grb10, and RasGAP (3, 35). It will be interesting to investigate whether these AKT/regulatory protein interactions mediated by the PH domain are also modulated by Ca^{2+} -CaM.

REFERENCES

1. Deb, T. B., Cotichchia, C. M., and Dickson, R. B. (2004) *J. Biol. Chem.* **279**, 38903–38911
2. Shen, X., Valencia, C. A., Szostak, J., Dong, B., and Liu, R. (2005) *Proc. Natl. Acad. Sci. U. S. A.* **102**, 5969–5974
3. Datta, K., Franke, T. F., Chan, T. O., Makris, A., Yang, S. I., Kaplan, D. R., Morrison, D. K., Golemis, E. A., and Tsichlis, P. N. (1995) *Mol. Cell. Biol.* **15**, 2304–2310



Interaction between Ca^{2+} /CaM and the PH Domain of AKT1

4. Staal, S. P., Hartley, J. W., and Rowe, W. P. (1977) *Proc. Natl. Acad. Sci. U. S. A.* **74**, 3065–3067
5. Staal, S. P. (1987) *Proc. Natl. Acad. Sci. U. S. A.* **84**, 5034–5037
6. Bellacosa, A., Testa, J. R., Staal, S. P., and Tsichlis, P. N. (1991) *Science* **254**, 274–277
7. Testa, J. R., and Bellacosa, A. (2001) *Proc. Natl. Acad. Sci. U. S. A.* **98**, 10983–10985
8. Kumar, C. C., and Madison, V. (2005) *Oncogene* **24**, 7493–7501
9. Downward, J. (2004) *Semin. Cell Dev. Biol.* **15**, 177–182
10. Brazil, D. P., and Hemmings, B. A. (2001) *Trends Biochem. Sci.* **26**, 657–664
11. Rossig, L., Jadidi, A. S., Urbich, C., Badorff, C., Zeiher, A. M., and Dimmeler, S. (2001) *Mol. Cell. Biol.* **21**, 5644–5657
12. Liu, Z., Zhou, X., Shapiro, S. D., Shipley, J. M., Twining, S. S., Diaz, L. A., Senior, R. M., and Werb, Z. (2000) *Cell* **102**, 647–655
13. Cross, D. A., Alessi, D. R., Cohen, P., Andjelkovich, M., and Hemmings, B. A. (1995) *Nature* **378**, 785–789
14. del Peso, L., Gonzalez-Garcia, M., Page, C., Herrera, R., and Nunez, G. (1997) *Science* **278**, 687–689
15. Datta, S. R., Dudek, H., Tao, X., Masters, S., Fu, H., Gotoh, Y., and Greenberg, M. E. (1997) *Cell* **91**, 231–241
16. Brunet, A., Bonni, A., Zigmond, M. J., Lin, M. Z., Juo, P., Hu, L. S., Anderson, M. J., Arden, K. C., Blenis, J., and Greenberg, M. E. (1999) *Cell* **96**, 857–868
17. Biggs, W. H., 3rd, Meisenhelder, J., Hunter, T., Cavenee, W. K., and Arden, K. C. (1999) *Proc. Natl. Acad. Sci. U. S. A.* **96**, 7421–7426
18. Kops, G. J., de Ruyter, N. D., De Vries-Smits, A. M., Powell, D. R., Bos, J. L., and Burgering, B. M. (1999) *Nature* **398**, 630–634
19. Cardone, M. H., Roy, N., Stennicke, H. R., Salvesen, G. S., Franke, T. F., Stanbridge, E., Frisch, S., and Reed, J. C. (1998) *Science* **282**, 1318–1321
20. Kane, L. P., Shapiro, V. S., Stokoe, D., and Weiss, A. (1999) *Curr. Biol.* **9**, 601–604
21. Ozes, O. N., Mayo, L. D., Gustin, J. A., Pfeffer, S. R., Pfeffer, L. M., and Donner, D. B. (1999) *Nature* **401**, 82–85
22. Romashkova, J. A., and Makarov, S. S. (1999) *Nature* **401**, 86–90
23. Scheid, M. P., and Woodgett, J. R. (2003) *FEBS Lett.* **546**, 108–112
24. Brazil, D. P., Yang, Z. Z., and Hemmings, B. A. (2004) *Trends Biochem. Sci.* **29**, 233–242
25. Bellacosa, A., Kumar, C. C., Di Cristofano, A., and Testa, J. R. (2005) *Adv. Cancer Res.* **94**, 29–86
26. Franke, T. F., Yang, S. I., Chan, T. O., Datta, K., Kazlauskas, A., Morrison, D. K., Kaplan, D. R., and Tsichlis, P. N. (1995) *Cell* **81**, 727–736
27. Chan, T. O., Rittenhouse, S. E., and Tsichlis, P. N. (1999) *Annu. Rev. Biochem.* **68**, 965–1014
28. Sarbassov, D. D., Guertin, D. A., Ali, S. M., and Sabatini, D. M. (2005) *Science* **307**, 1098–1101
29. Pommier, Y., Sordet, O., Antony, S., Hayward, R. L., and Kohn, K. W. (2004) *Oncogene* **23**, 2934–2949
30. Luo, J., Manning, B. D., and Cantley, L. C. (2003) *Cancer Cell* **4**, 257–262
31. Bjornsti, M. A., and Houghton, P. J. (2004) *Cancer Cell* **5**, 519–523
32. Mitsiades, C. S., Mitsiades, N., and Koutsilieris, M. (2004) *Curr. Cancer Drug Targets* **4**, 235–256
33. Altomare, D. A., and Testa, J. R. (2005) *Oncogene* **24**, 7455–7464
34. Testa, J. R., and Tsichlis, P. N. (2005) *Oncogene* **24**, 7391–7393
35. Du, K., and Tsichlis, P. N. (2005) *Oncogene* **24**, 7401–7409
36. McCullar, J. S., Larsen, S. A., Millimaki, R. A., and Filtz, T. M. (2003) *J. Biol. Chem.* **278**, 33708–33713
37. Yap, K. L., Kim, J., Truong, K., Sherman, M., Yuan, T., and Ikura, M. (2000) *J. Struct. Funct. Genomics* **1**, 8–14
38. Thomas, C. C., Deak, M., Alessi, D. R., and van Aalten, D. M. (2002) *Curr. Biol.* **12**, 1256–1262
39. Milburn, C. C., Deak, M., Kelly, S. M., Price, N. C., Alessi, D. R., and Van Aalten, D. M. (2003) *Biochem. J.* **375**, 531–538
40. Yang, J., Cron, P., Good, V. M., Thompson, V., Hemmings, B. A., and Barford, D. (2002) *Nat. Struct. Biol.* **9**, 940–944
41. Auguin, D., Barthe, P., Auge-Senegas, M. T., Stern, M. H., Noguchi, M., and Roumestand, C. (2004) *J. Biomol. NMR* **28**, 137–155
42. Rhoads, A. R., and Friedberg, F. (1997) *FASEB J.* **11**, 331–340
43. Torok, K., and Trentham, D. R. (1994) *Biochemistry* **33**, 12807–12820
44. Weinstein, H., and Mehler, E. L. (1994) *Annu. Rev. Physiol.* **56**, 213–236
45. Crivici, A., and Ikura, M. (1995) *Annu. Rev. Biophys. Biomol. Struct.* **24**, 85–116
46. Zielinski, R. E. (1998) *Annu. Rev. Plant Physiol. Plant Mol. Biol.* **49**, 697–725
47. Chin, D., and Means, A. R. (2000) *Trends Cell Biol.* **10**, 322–328
48. Saimi, Y., and Kung, C. (2002) *Annu. Rev. Physiol.* **64**, 289–311
49. Yang, T., and Poovaiah, B. W. (2003) *Trends Plant Sci.* **8**, 505–512
50. Lemmon, M. A., Ferguson, K. M., and Abrams, C. S. (2002) *FEBS Lett.* **513**, 71–76
51. Gao, T., Furnari, F., and Newton, A. C. (2005) *Mol. Cell* **18**, 13–24
52. Guilherme, A., Klarlund, J. K., Krystal, G., and Czech, M. P. (1996) *J. Biol. Chem.* **271**, 29533–29536
53. Maehama, T., and Dixon, J. E. (1998) *J. Biol. Chem.* **273**, 13375–13378
54. Maehama, T., Taylor, G. S., and Dixon, J. E. (2001) *Annu. Rev. Biochem.* **70**, 247–279
55. Meier, R., Alessi, D. R., Cron, P., Andjelkovic, M., and Hemmings, B. A. (1997) *J. Biol. Chem.* **272**, 30491–30497
56. Meier, R., and Hemmings, B. A. (1999) *J. Recept. Signal Transduct. Res.* **19**, 121–128
57. Andjelkovic, M., Alessi, D. R., Meier, R., Fernandez, A., Lamb, N. J., Frech, M., Cron, P., Cohen, P., Lucocq, J. M., and Hemmings, B. A. (1997) *J. Biol. Chem.* **272**, 31515–31524
58. Frech, M., Andjelkovic, M., Ingley, E., Reddy, K. K., Falck, J. R., and Hemmings, B. A. (1997) *J. Biol. Chem.* **272**, 8474–8481
59. Kavran, J. M., Klein, D. E., Lee, A., Falasca, M., Isakoff, S. J., Skolnik, E. Y., and Lemmon, M. A. (1998) *J. Biol. Chem.* **273**, 30497–30508
60. James, S. R., Downes, C. P., Gigg, R., Grove, S. J., Holmes, A. B., and Alessi, D. R. (1996) *Biochem. J.* **315**, 709–713